Analysis of conjugation of chloramphenicol and hemoglobin by fluorescence, circular dichroism and molecular modeling

ARTICLE *in* JOURNAL OF MOLECULAR STRUCTURE · JANUARY 2012

Impact Factor: 1.6 · DOI: 10.1016/j.molstruc.2011.10.022

6 AUTHORS, INCLUDING:

Fei Ding
Qingdao Agricultural University
34 PUBLICATIONS **405** CITATIONS
SEE PROFILE

Wei Liu
University of Science and Technology of Ch…
223 PUBLICATIONS **1,383** CITATIONS
SEE PROFILE

Ying Sun
Yale University
115 PUBLICATIONS **1,347** CITATIONS
SEE PROFILE

Journal of Molecular Structure 1007 (2012) 81–87

Contents lists available at SciVerse ScienceDirect

Journal of Molecular Structure

journal homepage: www.elsevier.com/locate/molstruc

Analysis of conjugation of chloramphenicol and hemoglobin by fluorescence, circular dichroism and molecular modeling

Fei Ding [a,b], Wei Liu [c], Ye Sun [a], Xin-Ling Yang [a], Ying Sun [d,*], Li Zhang [e,*]

[a] Department of Chemistry, China Agricultural University, Beijing 100193, China
[b] Department of Biological Engineering, Massachusetts Institute of Technology, Cambridge, MA 02139, United States
[c] College of Economics & Management, China Agricultural University, Beijing 100083, China
[d] College of Resources and Environmental Sciences, China Agricultural University, Beijing 100193, China
[e] Key Laboratory of Pesticide Chemistry and Application Technology, Ministry of Agriculture, Department of Applied Chemistry, China Agricultural University, Beijing 100193, China

ARTICLE INFO

Article history:
Received 10 June 2011
Received in revised form 12 October 2011
Accepted 13 October 2011
Available online 11 November 2011

Keywords:
Chloramphenicol
Hemoglobin
Albumin
Fluorescence
Molecular modeling

ABSTRACT

Chloramphenicol is a low cost, broad spectrum, highly active antibiotic, and widely used in the treatment of serious infections, including typhoid fever and other life-threatening infections of the central nervous system and respiratory tract. The purpose of the present study was to examine the conjugation of chloramphenicol with hemoglobin (Hb) and compared with albumin at molecular level, utilizing fluorescence, UV/vis absorption, circular dichroism (CD) as well as molecular modeling. Fluorescence data indicate that drug bind Hb generate quenching via static mechanism, this corroborates UV/vis absorption measurements that the ground state complex formation with an affinity of $10^4\ M^{-1}$, and the driving forces in the Hb-drug complex are hydrophilic interactions and hydrogen bonds, as derived from computational model. The accurate binding site of drug has been identified from the analysis of fluorescence and molecular modeling, $\alpha_1\beta_2$ interface of Hb was assigned to possess high-affinity for drug, which located at the β-37 Trp nearby. The structural investigation of the complexed Hb by synchronous fluorescence, UV/vis absorption, and CD observations revealed some degree of Hb structure unfolding upon complexation. Based on molecular modeling, we can draw the conclusion that the binding affinity of drug with albumin is superior, compared with Hb. These phenomena can provide salient information on the absorption, distribution, pharmacology, and toxicity of chloramphenicol and other drugs which have analogous configuration with chloramphenicol.

1. Introduction

Among pharmaceuticals, antibiotics, a word that contains an extensive spectrum of substances, are of special attention, the huge amounts of antibiotics applied in both human and veterinary medicine have brought about their concerns for public health [1]. Chloramphenicol, 2,2-dichlor-*N*-[(aR,bR)-b-hydroxy-a-hydroxymethyl-4-nitrophenethyl] acetamide, structure shown in Fig. 1, is a bacteriostatic antibiotic originally derived from the bacterium *Streptomyces venezuelae*, isolated by David Gottlieb and is now synthesized chemically, and introduced into clinical use in 1947 [2]. It is effective against an vast range of Gram-positive and Gram-negative bacteria in both humans and animals, and exerts its activity through inhibiting bacterial protein synthesis by binding at the 50S ribosomal subunit, therefore, interfering with the requisite peptidyl transferase [3]. Chloramphenicol is immensely utilized in the treatment of serious infections including typhoid fever and other forms of salmonellosis, in severe infections due to *Haemophilus influenza*, and in other life-threatening infections of the central nervous system and respiratory tract [3]. It is rapidly absorbed and distributed in organs and edible tissues after oral and parenteral administration [4]. Epidemiological results have shown that it can lead to grave adverse effects in humans, such as mild anemia with reticulocytopenia, sometimes followed by leucopenia and thrombocytopenia and aplastic anemia [5]. The suspected carcinogenity of chloramphenicol is also thought to be dosage independent [6]. For these reasons this drug has been prohibited for the use in humans within the United States and European Union since 1994, except humans for life-threatening illness that resistant to other antibiotics [7]. Today, the drug is still widely used in developing countries, particularly in Asia, in patients of all age groups because it is exceedingly inexpensive, broad spectrum antibiotic, and readily available. For example, the incidence of fatal aplastic anemia in China is two cases per 100,000 and in Thailand 3.7 cases per 100,000 [8].

It is generally believed nowadays that only the unbound form of a drug in plasma is available to produce a pharmacological action, thus, characterization of drug binding to plasma protein is of utmost importance for drug discovery and preclinical studies of drug

* Corresponding authors. Tel./fax: +86 10 62734676.
E-mail addresses: sunying@cau.edu.cn (Y. Sun), zhli.work@gmail.com (L. Zhang).

0022-2860/$ - see front matter © 2011 Elsevier B.V. All rights reserved.
doi:10.1016/j.molstruc.2011.10.022

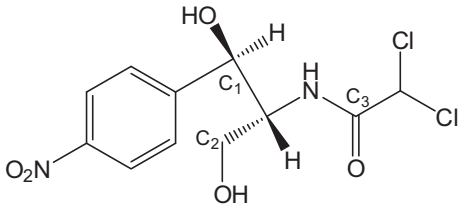

Fig. 1. Molecular structure of chloramphenicol.

candidates in pharmaceutical research [9]. The affinity of a drug toward plasma protein is an important issue when determining its overall therapeutic, pharmacokinetic, and toxicological outline, as well as being central to comprehend the distribution and biotransformation approaches of a drug in the human body [10]. This association can occur with a variety of ingredients in blood, including proteins such as hemoglobin (Hb). Hb is an essential component of the circulatory system of vertebrates, and the concentration of Hb in the plasma of human adults around 330 mg mL^{-1}. The molecular weight of Hb is 64.45 kDa and its high-resolution atomic structure has been elucidated by Perutz [11], which is one of the major breakthroughs in the history of molecular biology. Hb is roughly spherical molecule $6.4 \times 5.5 \times 5.0$ nm, it is a tetrameric protein containing four heme groups, each one associated with each polypeptide chain to which oxygen and several other small molecules can bind reversibly [12]. In adult human Hb, there are two identical chains of 141 amino acids, the α-chains, and two identical β-chains, each of 146 residues. The α-chains contain seven and the β-chains eight helices [12]. The tetrameric nature of Hb is crucial to its biological function. Drug associations at protein binding level will in most cases evidently influence the apparent distribution volume of the drugs and affect the elimination rate of drugs. It can be announced that the effectiveness of drugs as pharmaceutical agents is rely on their binding ability and can also alter the drug stability and toxicity during the treatment [13]. Therefore, the clue on the conjugation of protein and drugs can make us better understand the absorption and distribution of drugs *in vivo*, and have great significance in pharmacology, biopharmaceutics, biochemistry, immunochemistry, and related fields.

There are numerous techniques available for probing the extent of plasma protein binding, e.g. equilibrium dialysis, ultrafiltration, ultracentrifugation, fluorescence, capillary electrophoresis, surface plasmon resonance, calorimetry, surface tension, chromatography, crystallology, and nuclear magnetic resonance [14–17], however, fluorescence is often the approach of choice due to the production of most comprehensively qualitative and quantitative information on the protein–drug complexation [18]. The objective of the current work was to use photophysical techniques, i.e. fluorescence, UV/vis absorption, CD, in combination with molecular modeling, to characterize the potential noncovalent binding of chloramphenicol to Hb. Utilizing molecular modeling simulations, we have also compared the association of chloramphenicol with albumin, since albumin is capable of binding to a diverse range of pharmaceuticals, including chloramphenicol. Through this work, we expect it can offer a further insight of the complexation will enable distinct interpretations for the pharmacological and toxicological activities of chloramphenicol.

2. Materials and methods

2.1. Materials

Hemoglobin human (H7379, lyophilized powder) and chloramphenicol (C0378, $\geqslant$98%) were obtained from Sigma–Aldrich (USA) and used without further purification. Milli-Q ultrapure water (Millipore, USA) was used throughout the experiments. All the experiments were performed in Tris (0.2 M)-HCl (0.1 M) buffer of pH = 7.4, with an ionic strength 0.1 in the presence of NaCl, except where specified, and the pH was checked with a suitably standardized Orion-868 pH meter (Thermo Scientific, USA). Dilutions of the Hb stock solution (30 μM) in Tris–HCl buffer were prepared immediately before use, and the concentration of Hb was determined spectrophotometrically using ε_{555} nm = 12.5 mM^{-1} cm^{-1} per heme [19]. All other reagents employed were of analytical grade and received from Sigma–Aldrich.

2.2. Methods

2.2.1. Fluorescence emission

Fluorescence emission spectra were recorded with a 1.0 cm path length quartz cell using a F-4500 spectrofluorimeter (Hitachi, Japan) equipped with a thermostatic bath. The excitation and emission slits were set at 5.0 nm each, intrinsic fluorescence was acquired by exciting the stirred protein solution at 280 nm, and the emission spectra were measured in the wavelength range of 300–450 nm at a scanning speed of 240 nm min^{-1}. The reference sample consisting of the Tris–HCl buffer of chloramphenicol did not give any fluorescence signal. The fluorescence intensities were corrected for absorption of the exciting light and reabsorption of the emitted light to decrease the inner filter effect by using the following relationship [20]:

$$F_{cor} = F_{obs} \times e^{\frac{A_{ex}+A_{em}}{2}} \quad (1)$$

where F_{cor} and F_{obs} are the fluorescence intensities corrected and observed, respectively, and A_{ex} and A_{em} are the absorption of the systems at the excitation and the emission wavelength, respectively. The fluorescence intensity utilized in this work is the corrected intensity.

2.2.2. Molecular modeling

Molecular modeling of the Hb-chloramphenicol conjugation was executed on SGI Fuel Workstation. The crystal structure of Hb was downloaded from Brookhaven Protein Data Bank (entry codes 1GZX, resolution 2.1 Å, http://www.rcsb.org/pdb). The two-dimensional structure of chloramphenicol was downloaded from PubChem (http://pubchem.ncbi.nlm.nih.gov). The potential of the three-dimensional structure of Hb was assigned according to the AMBER force field with Kollman all-atom charges. The initial structure of chloramphenicol was generated by molecular modeling software Sybyl 7.3. The geometry of the molecule was subsequently optimized to minimal energy using the Tripos force field with Gasteiger–Hückel charges, and the Surflex docking program was applied to calculate the possible conformation of the drug that binds to the protein [21].

2.2.3. UV/vis absorption spectra

UV/vis absorption spectra were carried out on a Lambda-25 double-beam spectrophotometer (Perkin–Elmer, USA) at room temperature in the range of 250–500 nm using a quartz cuvette with 1.0 cm path length.

2.2.4. CD spectra

Far-UV CD spectra were examined with a Jasco-810 spectropolarimeter (Jasco, Japan) equipped with a microcomputer, the instrument was calibrated with d-10-camphorsulfonic acid. All the CD spectra were collected at 298 K with a thermostatically controlled cell holder attached to a Neslab RTE-110 water bath with an accuracy of ±0.1 °C. Each spectrum was gathered with use of a quartz cuvette of 0.2 cm path length and taken at wavelengths between

200 and 260 nm with 0.1 nm step resolution and averaged over five scans picked at a speed of 20 nm min^{-1} and response time of 1 s. All observed CD spectra were baseline subtracted for buffer and the secondary structure was computed exploiting Jasco standard spectra analysis software package, which calculates the different designations of secondary structures by comparison with CD spectra, determined from distinct proteins for which high-quality X-ray diffraction data are available [22]. The software is supplied in CDPro package which is obtainable at the web: http://lamar.colostate.edu/~sreeram/CDPro.

2.2.5. Statistical analysis

All assays were performed in $n = 3$ repetitions, the mean values, standard deviations, and statistical differences were evaluated utilizing analysis of variance (ANOVA). The mean values were compared using student's *t*-test, and all statistic data were processed using the OriginPro Software (OriginLab Corporation, USA).

3. Theory and calculation

3.2. Principles of fluorescence quenching [20]

Fluorescence quenching refers to any process that decreases the fluorescence intensity of a sample. A variety of molecular interactions can result in quenching. These include excited state reactions, molecular rearrangements, energy transfer, ground state complex formation, and collisional quenching. Fluorescence quenching is described by the Stern–Volmer equation:

$$\frac{F_0}{F} = 1 + k_q\tau_0[Q] = 1 + K_{SV}[Q] \quad (2)$$

In this equation F_0 and F are the fluorescence intensities in the absence and presence of quencher, respectively, k_q is the bimolecular quenching constant, τ_0 is the lifetime of the fluorophore in the absence of quencher, [Q] is the concentration of quencher, and K_{SV} is the Stern–Volmer quenching constant. Therefore, Eq. (2) was applied to determine K_{SV} by linear regression of a plot of F_0/F *against* [Q].

A linear Stern–Volmer plot is generally indicative of a single class of fluorophores in a protein, all equally accessible to the quencher. In many instances the fluorophore can be quenched both by collisions and by complex formation with the same quencher. The characteristic feature of the Stern–Volmer plots in such circumstances is an upward curvature, concave towards the *y*-axis, and F_0/F is related to [Q] by the modified form of the Stern–Volmer equation:

$$\frac{F_0}{F} = (1 + K_D[Q])(1 + K_S[Q]) \quad (3)$$

where K_D and K_S are the dynamic and static quenching constants. This modified form of the Stern–Volmer equation is the second order in [Q], which accounts for the upward curvature observed when both static and dynamic quenching occur for the same fluorophore. It is important to recognize that quenching can also transpire as a result of the formation of a non-fluorescent ground state complex between the fluorophore and quencher, this complex absorbs light and then immediately returns to the ground state without the emission of a photon, which is corresponding to a static mechanism. In this case, the bimolecular quenching constant is calculated and compared to the maximum value possible for diffusion-limited quenching in water ($\sim 10^{10}$ M^{-1} s^{-1}). There have been several literatures reporting that Hb quenching because of specific interaction, and the quenching constant has been several magnitudes larger than the maximum value of diffusion-limited quenching in water [23–26].

3.3. Calculation of association constant

When ligand molecules bind independently to a set of equivalent sites on a macromolecule, the equilibrium between free and bound ligand molecules is given by the following relation [23]:

$$\log\frac{F_0 - F}{F} = \log K + n\log[Q] \quad (4)$$

where F_0 and F are the fluorescence intensities in the absence and presence of quencher, respectively, K and n are the association constant and the number of binding sites, respectively, [Q] is the concentration of quencher. Thus, a plot of $\log(F_0 - F)/F$ *against* $\log[Q]$ can be used to calculate K and n.

4. Results and discussion

4.1. Fluorescence binding studies

Fig. 2 expresses the fluorescence emission spectra of Hb with various concentrations of chloramphenicol following an excitation at 280 nm, the working concentration of Hb utilized was 3.0 μM so as to prevent quenching of tryptophan (Trp) fluorescence by the neighboring heme group [27]. Hb displays a weak fluorescence emission band at 332 nm and its fluorescence intensity decreased regularly with the addition of chloramphenicol, accompanying by bathochromic effect (from 332 nm to 336 nm). Under the experimental conditions, chloramphenicol shows no fluorescence signal in the range 300–500 nm which did not interfere with Hb fluorescence. Hb is a globular tetrameric protein involves four globin chains, of which two are α-chains and two are β-chains. The tetramer is assembled from two αβ dimers, each αβ dimer contains three Trp residues, adding to a total of six Trp residues, namely α-14 Trp, β-15 Trp, and β-37 Trp [12]. Alpert et al. certified that the intrinsic fluorescence of Hb primarily originates from the β-37 Trp at the $\alpha_1\beta_2$ interface and serves as a reporter for R–T transition [28]. The R form is the oxy/ligand bound form while the T form is the deoxy form [29] and R–T form represent significant changes in relative fluorescence intensity. Consequently, the quenching of the intrinsic fluorescence of Hb clearly denoted that the association of chloramphenicol with Hb, chloramphenicol situated near the β-37 Trp residue, and the hydrophobicity of β-37 Trp was dropped [25].

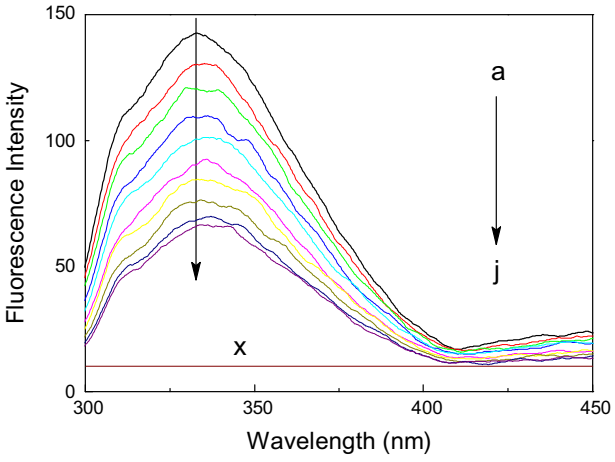

Fig. 2. Fluorescence emission spectra of Hb with various concentrations of chloramphenicol (pH = 7.4, T = 297 K). (a) 3.0 μM Hb, (b) → (j) 3.0 μM Hb in the presence of 5.0, 10, 15, 20, 25, 30, 35, 40, 45 μM chloramphenicol; (*x*) 45 μM chloramphenicol alone.

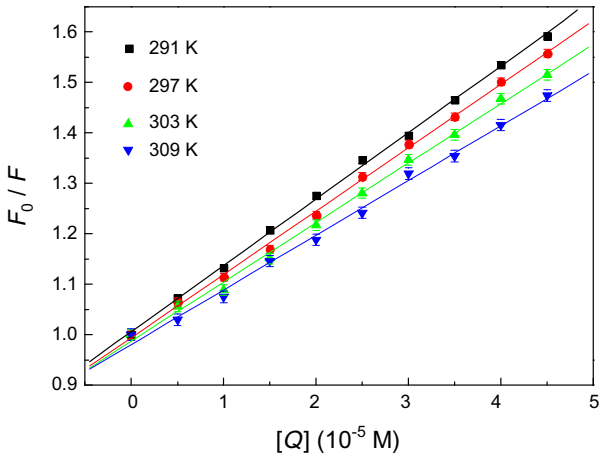

Fig. 3. Stern–Volmer plots displaying fluorescence quenching of Hb (3.0 μM) in the presence of different concentrations of chloramphenicol. Each data was the mean of three separate experiments ± standard deviation (SD) ranging 0.64–1.14%.

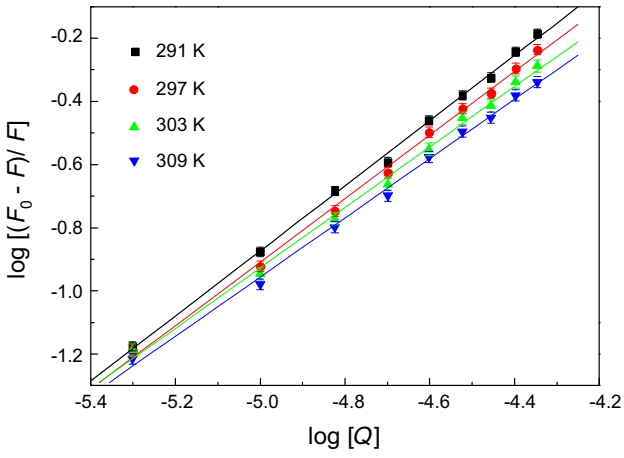

Fig. 4. The plots of $\log(F_0 - F)/F$ *versus* $\log[Q]$ for the Hb-chloramphenicol, data was the mean of three independent observations ± SD ranging 1.44–1.94%.

Table 1
Stern-Volmer quenching constants for chloramphenicol binding to Hb determined by fluorescence quenching.

T (K)	K_{SV}[a] ($\times 10^4$ M^{-1})	k_q ($\times 10^{12}$ M^{-1} s^{-1})	R[b]
291	1.316 ± 0.006	1.316 ± 0.006	0.9996
297	1.255 ± 0.008	1.255 ± 0.008	0.9993
303	1.176 ± 0.011	1.176 ± 0.011	0.9985
309	1.083 ± 0.011	1.083 ± 0.011	0.9979

[a] The mean value of three individual experiments with standard deviation (S.D.) ± 0.63% to 1.05%.
[b] R is the correlation coefficient.

Table 2
Association constants for chloramphenicol bound per Hb molecule

T (K)	K[a] ($\times 104$ M^{-1})	n	R[b]
291	1.909 ± 0.014	1.03	0.9991
297	1.324 ± 0.016	1.01	0.9989
303	0.7194 ± 0.019	0.96	0.9982
309	0.5408 ± 0.017	0.94	0.9985

[a] Data represent averages of triplicate measurements from each fluorescence quenching with S.D. ranging 1.43% - 1.94%.
[b] R is the correlation coefficient.

To elucidate the data from fluorescence quenching, it is necessary to check what kind of reaction takes place between chloramphenicol and Hb. In this case, Stern–Volmer Eq. (2) was applied for data analysis, Fig. 3 means the Stern–Volmer plots of F_0/F *versus* [Q] at the four different temperatures, and the calculated K_{SV} and k_q values were presented in Table 1. The results hint Stern–Volmer quenching constants K_{SV} are inversely correlated with temperature and the values of k_q are much greater than the maximum scattering collisional quenching constant ($\sim 10^{10}$ M^{-1} s^{-1}), suggesting the probable quenching mechanism of Hb fluorescence by chloramphenicol is essentially a static type.

Fig. 4 indicates the plots of $\log(F_0 - F)/F$ *against* $\log[Q]$ for the Hb-chloramphenicol system at different temperatures and the corresponding outcomes of K and n values were listed in Table 2. The data appear the association constants K are reduced with the rising temperature, which alluded the forming of an unstable compound in the reaction, the unstable compound would be partly decomposed when the temperature increased. The value of n is approximately equal to 1, which may imply the existence of just one single binding site in Hb for chloramphenicol. A valuable feature of intrinsic fluorescence of Hb is owing to the β-37 Trp at the $\alpha_1\beta_2$ interface [28], from the value of n, chloramphenicol binding domain most likely close to this Trp residue, and causing fluorescence quenching in the complexation.

4.2. Molecular modeling

In order to harvest a better understanding on the binding location for chloramphenicol on Hb, molecular modeling simulations were conducted to complement the experiments in solution, and best docking energy result is shown in Fig. 5. As can be seen, chloramphenicol binding site is located within active cavity constituted by α_1, β_2, and α_2 subunits, which revealed that hydrophilic interactions plays important role between chloramphenicol and Hb. The association between drug and Hb is not exclusively hydrophilic interaction in nature, because there are four polar residues in the proximity of the chloramphenicol acting major role in stabilizing chloramphenicol by hydrogen bonds. For example, the hydrogen atom and oxygen atom of hydroxyl group in C_1, and the oxygen atom of nitryl in chloramphenicol can make hydrogen bonds with oxygen atom in Asp-526, hydrogen atom in Arg-141, hydrogen atoms of hydroxyl group in Ser-533 and Ser-502 residues, the bond length, respectively, is 1.89 Å, 2.11 Å, 2.01 Å, and 1.94 Å. The hydrogen bonds act as an "anchor", which extremely determines the three-dimensional space position of chloramphenicol in the active pocket, and stimulates the hydrophilic interactions of the chloramphenicol with the side chain of protein [30]. Furthermore, the molecular distance between the chloramphenicol and the Trp-580 (namely Trp-37) residue in the β_2 chain is very close, which confirm the fluorescence emission analyses that chloramphenicol near the β-37 Trp residue, and induce structural changes of Hb upon complexation with chloramphenicol.

4.3. Synchronous fluorescence

Synchronous fluorescence involves simultaneous scanning of the excitation and emission monochromators while maintaining a constant wavelength interval ($\Delta\lambda$) or fixed increment of energy ($\Delta\nu$) between them [31]. According to the theory of Miller [32], when $\Delta\lambda$ = 15 or 60 nm, the characteristic information of Tyr or Trp residues was observed. Fig. 6 shows the synchronous fluorescence of Hb in Tris–HCl buffer in the presence of different amounts of chloramphenicol. A slight red shift can be noted from Fig. 6

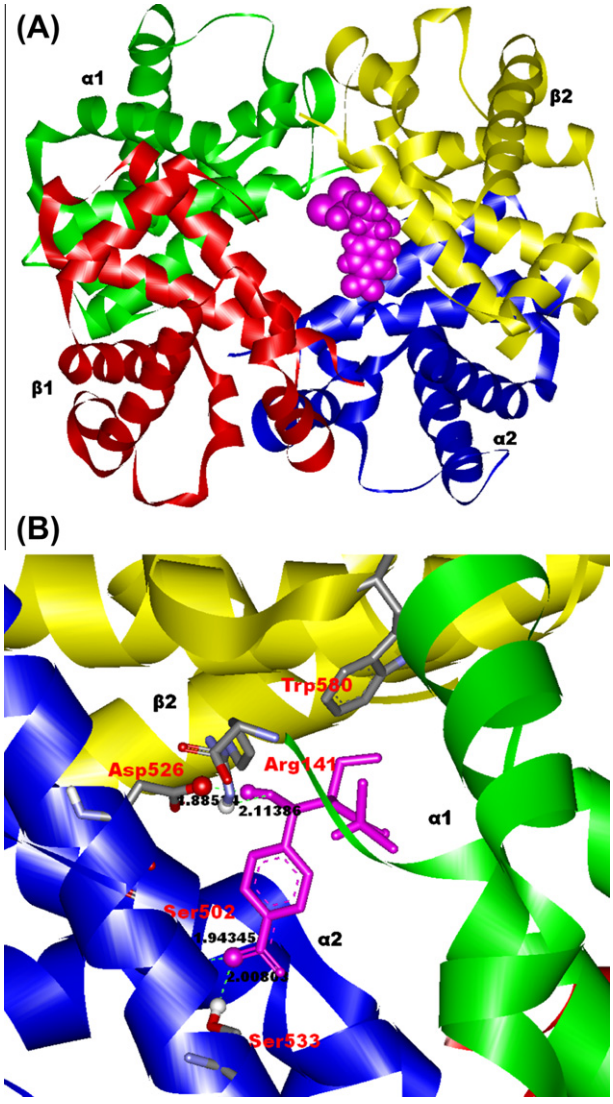

Fig. 5. Molecular modeling of chloramphenicol docked to Hb. Panel (A) shows docked chloramphenicol into Hb at the cavity composed of α_1, β_2, and α_2 subunits, Hb represented in surface colored in green (α_1 chain), yellow (β_2), red (β_1), and blue (α_2), to chloramphenicol, colored in magenta. Panel (B) depicts the amino acid residues involved in binding of chloramphenicol. The magenta ball-and-stick model indicates chloramphenicol molecule, the crucial amino acid residues around chloramphenicol has been displayed in stick model, gray color stick model expresses the Arg-141, Ser-502, Asp-526, Ser-533, and Trp-580 residues, and the hydrogen bonds between chloramphenicol and Hb denoted using green dash line. (For interpretation of the references to color in this figure legend, the reader is referred to the web version of the article.)

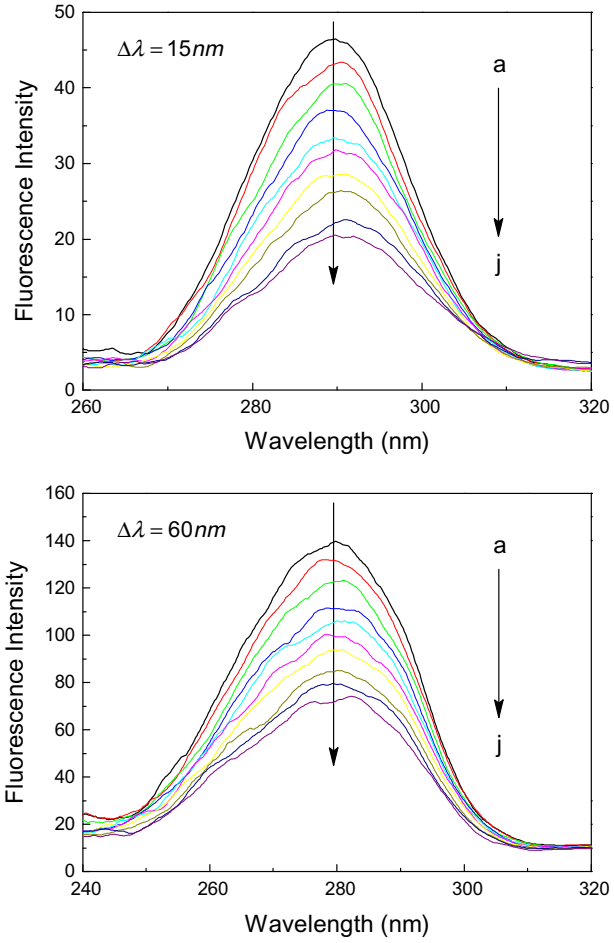

Fig. 6. Synchronous fluorescence spectra of Hb (3.0 μM) in the presence of different concentrations of chloramphenicol, (a → j):*c* (chloramphenicol) = 0, 5.0, 10, 15, 20, 25, 30, 35, 40, 45 μM; pH = 7.4, *T* = 297 K.

when $\Delta\lambda$ = 15 or 60 nm (Tyr: 289 nm → 291 nm; Trp: 279 nm → 282 nm), which evidenced that the hydrophilicity around the Tyr and Trp was rised and the hydrophobicity lowered, on account of the change in microenvironment with the insertion of chloramphenicol. As mentioned above, intrinsic fluorescence of Hb is chiefly due to the β-37 Trp at the $\alpha_1\beta_2$ interface, though it may include some contribution by the surface Trp residues, α-14 and β-15 Trp residues. Moreover, aromatic residues such as α-42 Tyr, α-140 Tyr, and β-145 Tyr are located at the $\alpha_1\beta_2$ subunit interface and experience alters of environment with the quaternary structure transition from T to R [33], the bathochromatic shift is consistent with a rearrangement of tertiary structure of Tyr residues during the binding process. These phenomena illustrated that chloramphenicol aroused tertiary structural changes in the microenvironment of β-37 Trp and some Tyr residues at the $\alpha_1\beta_2$ interface, from hydrophobic to polar environment.

4.4. UV/vis absorption spectra

UV/vis absorption measurement is a simple method and applicable to explore the structural change and know the complex formation, Fig. 7 expresses the electronic absorption spectra of Hb from 250 nm to 500 nm in Tris–HCl buffer in the presence of various amounts of chloramphenicol. The absorption peak at 273 nm due to phenyl group of Trp and Tyr residues and a sharp peak at 406 nm owing to the Soret absorption by the heme system [34]. The addition of chloramphenicol results in the UV absorption intensity of Soret band decreased while the maximum peak position remains unchanged, which proclaimed there exists interaction between chloramphenicol and Hb. The occurrence of isosbestic point at 305 nm may demonstrate the presence of bound and free chloramphenicol in equilibrium [35], in other words, an isosbestic point was considered as a direct proof for Hb-chloramphenicol complex formation.

4.5. CD spectra

To quantitative analysis the structural changes of Hb, the raw CD spectra of Hb in the absence and presence of chloramphenicol were scanned in Fig. 8, and secondary structure calculated based on raw CD data summarized in Table 3. The CD spectra of Hb displayed two negative peaks in the far-UV region at 208 and

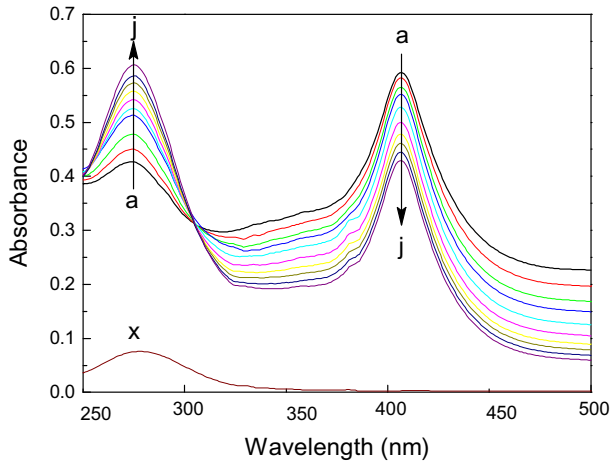

Fig. 7. UV/vis absorption spectra of Hb (3.0 μM) in the presence of different concentrations of chloramphenicol, (a → j):*c* (chloramphenicol) = 0, 3.0, 6.0, 9.0, 12, 15, 18, 21, 24, 27 μM; (*x*) 3.0 μM chloramphenicol only; pH = 7.4, *T* = 297 K.

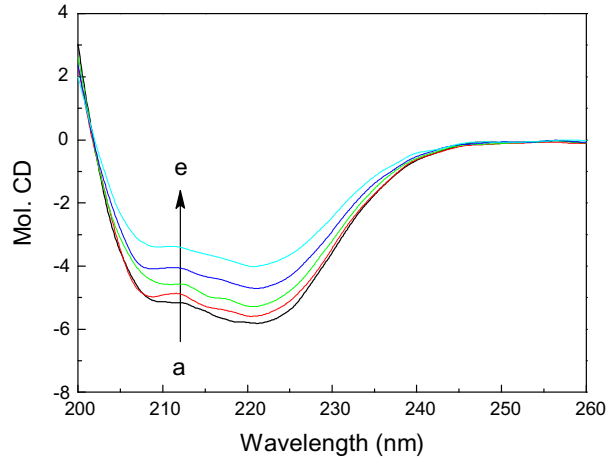

Fig. 8. Far-UV CD spectra of the Hb-chloramphenicol system. (a) 3.0 μM Hb, (b) → (e) 3.0 μM Hb in the presence of 3.0, 6.0, 12, 24 μM chloramphenicol; pH = 7.4, *T* = 298 K.

222 nm, typical of α-helical structure of protein. The reasonable explanation is that the negative peaks between 208 and 209 nm, and 222 and 223 nm are both contributed by $n \rightarrow \pi^*$ transition for the peptide bond of α-helix [36]. Free Hb has 78.6% α-helix, 1.9% β-sheet, 6.3% turn, and 13.2% random coil, upon association with chloramphenicol, reduction of α-helix was observed from 78.6% free Hb to 71.3% Hb-chloramphenicol complex while increase in β-sheet, turn, and random coil from 1.9%, 6.3%, and 13.2% free Hb to 3.5%, 10.1%, and 15.1% Hb-chloramphenicol complex at a molar ratio of Hb to chloramphenicol of 1:8. The decrease of α-helix with an increase in the β-sheet, turn, and random coil manifesting chloramphenicol bound with the amino acid residue of the polypeptide chain and thus giving rise to some degree of unfolding of Hb [37]. The structural changes detected by CD spectra are in agreement with synchronous fluorescence, UV/vis absorption, and also molecular modeling results.

4.6. Comparison with albumin

There are some reports indicating chloramphenicol can complex with albumin [38–42], in our previous work, we also explained that chloramphenicol binding to subdomain IIA in HSA,

Table 3
Secondary structures of Hb complexes with chloramphenicol at pH 7.4 computed by CDSSTR software

c(chloramphenicol) (μM)	Secondary structure components (%)			
	α-helix (±1%)	β-sheet (±1%)	Turn (±2%)	Random (±1%)
0	78.6	1.9	6.3	13.2
3.0	77.5	2.1	6.7	13.7
6.0	75.7	2.4	7.7	14.2
12.0	73.6	2.9	8.8	14.7
24.0	71.3	3.5	10.1	15.1

and Förster energy transfer occurs [43], in the present paper, we sought to enlarge the above outcomes to detailed assess the HSA binding manner of chloramphenicol employing molecular modeling approach method below. The best docking energy result is shown in Fig. 9 (entry codes 1H9Z, resolution 2.5 Å), chloramphenicol binding site is situated within subdomain IIA in Sudlow's site I

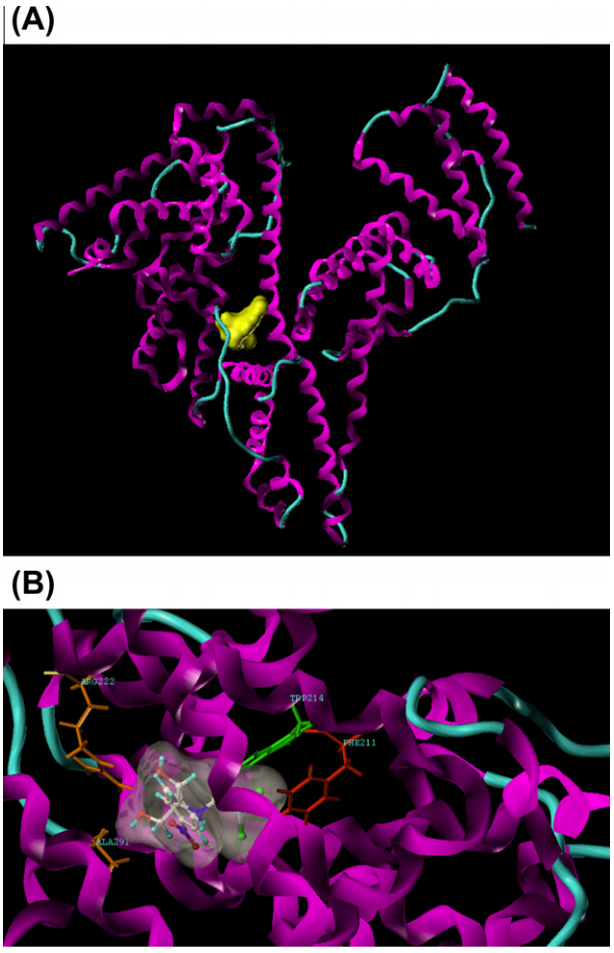

Fig. 9. Molecular modeling of chloramphenicol docked to HSA. Panel (A) shows docked chloramphenicol into HSA at subdomain IIA, HSA represented in surface colored in purple, to chloramphenicol, colored in yellow. Panel (B) depicts the amino acid residues involved in binding of chloramphenicol. The ball-and-stick model indicates chloramphenicol molecule, colored as per the atoms and possess white surface of van der Waals radius. The crucial amino acid residues around chloramphenicol has been displayed in stick model, red color stick model states hydrophobic interactions between the Phe-211 residue and two chlorine atoms of chloramphenicol; orange color stick model denotes hydrogen bonds between the Arg-222 and Ala-291 residues and chloramphenicol; green color stick model expresses π–π interactions between the Trp-214 and chloramphenicol. (For interpretation of the references to color in this figure legend, the reader is referred to the web version of the article.)

formed by six-helices [44], two chlorine atoms of chloramphenicol toward the benzene ring in the Phe-211, which implied that hydrophobic interaction running notable function between them. The oxygen atom of hydroxyl group in C_1 and C_2, and hydrogen atom of hydroxyl group in C_2 can generate hydrogen bonds with the hydrogen atom of amino group in Arg-222, and oxygen atom of carbonyl group in Ala-291, the bond length is 2.24 Å, 1.987 Å, and 1.829 Å, respectively. In addition, the perpendicular molecular distance between the nucleus of benzene ring in chloramphenicol and the heart of benzene ring in Trp-214 is 5.192 Å, as a result, evincing the existence of evident π–π interactions between drug and HSA, and corroborates with the approximate distance derived from Förster theory. In view of the molecular modeling results, it is obvious that the hydrophobic interaction, hydrogen bond, and π–π interaction between drug and HSA was greater than drug conjugates with Hb, this outcome based on computational analyses were in agreement with experiments in solution, i.e. the binding affinity of chloramphenicol with HSA is superior, compared with Hb.

5. Concluding remarks

Chloramphenicol is a highly active, broad spectrum antibiotic, with excellent antibacterial and pharmacokinetic properties. The therapeutic dose of chloramphenicol is normally 50 mg kg^{-1} daily, in divided doses, and the time periods of therapy are often 10–15 days [45]. However, accumulating evidences have proved it can bring about dangerous adverse effects in humans such as aplastic anemia, which is commonly fatal. The present task has stated clearly that the conjugation of chloramphenicol to Hb under simulated physiological conditions, which were uncovered by amalgamating with fluorescence, UV/vis absorption, CD, and molecular modeling techniques. The results indicate that the fluorescence quenching of Hb was mainly originated from the static type, this coincides with the UV/vis absorption measurements demonstrating that the Hb-chloramphenicol ground state complex formation, chloramphenicol binds to Hb near the β-37 Trp at the $\alpha_1\beta_2$ interface with an affinity of 10^4 M^{-1}. The outcomes of fluorescence and molecular modeling illustrated that chloramphenicol was located within $\alpha_1\beta_2$ interface of Hb, and quenching the intrinsic fluorescence of β-37 Trp, thereby the structural alters of Hb was observed, i.e. some extent of Hb unfolding upon chloramphenicol complexation, as derived from synchronous fluorescence, UV/vis absorption, and CD spectra. In addition, it seemed rational to deduce that the antibiotic chloramphenicol, after oral and parenteral administration, the affinity of HSA with drug is greater than Hb.

Even though our jobs do not correlate directly *in vivo* bioassays, it casts central insight to the conjugation of the protein with antibiotic, chloramphenicol. For plasma proteins are undoubtedly the most important transporter of drugs and the affinity of a drug toward plasma proteins is a key topic when determining its total pharmacokinetic profile. In specific, the picked data emerged in this essay highlights for the first time how binding dynamics and which binding region can control for the chloramphenicol, because the concentration of Hb in plasma is much higher than albumin ($\sim$40 mg mL^{-1}) [46], it is irrational to neglect the drugs' complexation with Hb. Human epidemiological data explained that chloramphenicol has serious side effects on the haemopoietic system in humans, yet it would take a long time before any drug could ever replace chloramphenicol, since both its extensive use, effective, and it extremely low cost.

Acknowledgements

We are indebted to Professor Ulrich Kragh-Hansen of Department of Medical Biochemistry, University of Aarhus, for the priceless gift of his doctoral dissertation. We are grateful to Dr. Xiu-Nan Li of Institute of Process Engineering, Chinese Academy of Sciences, for his constant support during the CD measurements. Thanks also go to the reviewers of this paper for their precious suggestions. This work was funded by grant support from the National Science and Technology Support Program (No. 2011BAE06B05-5), the National Natural Science Foundation of China (No. 31171693), and the Chinese Universities Scientific Fund (Grant No. 2011JS034).

References

[1] A.J. Alanis, Arch. Med. Res. 36 (2005) 697.
[2] D. Gottlieb, H.W. Anderson, Science 107 (1948) 172.
[3] Q.D. You, S.X. Peng, Medicinal Chemistry, 2nd ed., Chemical Industry Press, Beijing, 2008.
[4] M.X. Jiang, Handbook of Medicinal Chemistry, Second ed., Science Press, Beijing, 2005.
[5] A.A. Yunis, Ann. Rev. Pharmacol. Toxicol. 28 (1988) 83.
[6] L. Santos, J. Barbosa, M.C. Castilho, F. Ramos, C.A.F. Ribeiro, M.I.N. da Silveira, Anal. Chim. Acta 529 (2005) 249.
[7] M.J. Bogusz, H. Hassan, E. Al-Enazi, Z. Ibrahim, M. Al-Tufail, J. Chromatogr. B 807 (2004) 343.
[8] S. Issaragrisil, D.W. Kaufman, T. Anderson, K. Chansung, T. Thamprasit, J. Sirijirachai, A. Piankijagum, Y. Porapakkham, S. Vannasaeng, P.E. Leaverton, S. Shapiro, N.S. Young, Blood 89 (1997) 4034.
[9] B. Meunier, A. Robert, Acc. Chem. Res. 43 (2010) 1444.
[10] R. Janzen, M. Schwarzer, M. Sperling, M. Vogel, T. Schwerdtle, U. Karst, Metallomics 3 (2011) 847.
[11] M.F. Perutz, M.G. Rossmann, A.F. Cullis, H. Muirhead, G. Will, A.C.T. North, Nature 185 (1960) 416.
[12] M.M. Cox, G.N. Phillips Jr, Handbook of Proteins: Structure, Function and Methods, vol. 2, John Wiley & Sons Ltd., West Sussex, 2007.
[13] V. Thilakarathne, V.A. Briand, Y.X. Zhou, R.M. Kasi, C.V. Kumar, Langmuir 27 (2011) 7663.
[14] P. Mandal, M. Bardhan, T. Ganguly, J. Photochem. Photobiol. B: Biol. 99 (2010) 78.
[15] S. Nagatomo, M. Nagai, T. Kitagawa, J. Am. Chem. Soc. 133 (2011) 10101.
[16] N. Seedher, S. Bhatia, Pharmacol. Res. 54 (2006) 77.
[17] B. Chakraborty, S. Basu, J. Lumin. 129 (2009) 34.
[18] P.C. Hebert, L.A. MacManus-Spencer, Anal. Chem. 82 (2010) 6463.
[19] A.A. Romeo, J.A. Capobianco, A.M. English, J. Am. Chem. Soc. 125 (2003) 14370.
[20] J.R. Lakowicz, Principles of Fluorescence Spectroscopy, third ed., Springer Science + Business Media, New York, 2006.
[21] A.N. Jain, J. Med. Chem. 46 (2003) 499.
[22] N. Sreerama, R.W. Woody, Meth. Enzymol. 383 (2004) 318.
[23] S.N. Khan, B. Islam, R. Yennamalli, Q. Zia, N. Subbarao, A.U. Khan, J. Pharm. Biomed. Anal. 48 (2008) 1096.
[24] P. Mandal, T. Ganguly, J. Phys. Chem. B 113 (2009) 14904.
[25] M. Mahato, P. Pal, T. Kamilya, R. Sarkar, A. Chaudhuri, G.B. Talapatra, J. Phys. Chem. B 114 (2010) 7062.
[26] S. Chaudhuri, S. Chakraborty, P.K. Sengupta, Biophys. Chem. 154 (2011) 26.
[27] R.E. Hirsch, R.L. Nagel, J. Biol. Chem. 256 (1981) 1080.
[28] B. Alpert, D.M. Jameson, G. Weber, Photochem. Photobiol. 31 (1980) 1.
[29] M.F. Perutz, G. Fermi, D.J. Abraham, C. Poyart, E. Bursaux, J. Am. Chem. Soc. 108 (1986) 1064.
[30] F. Zsila, Z. Bikádi, M. Simonyi, Bioorg. Med. Chem. 12 (2004) 3239.
[31] J.B.F. Lloyd, Nat. Phys. Sci. 231 (1971) 64.
[32] J.N. Miller, Proc. Analyt. Div. Chem. Soc. 16 (1979) 203.
[33] J. Baldwin, C. Chothia, J. Mol. Biol. 129 (1979) 175.
[34] H.R. Vardapetyan, A.S. Martirosyan, S.G. Tiratsuyan, A.A. Hovhannisyan, J. Photochem. Photobiol. B: Biol. 101 (2010) 53.
[35] A.G. Salvay, J.R. Grigera, M.F. Colombo, Biophys. J. 84 (2003) 564.
[36] N.J. Greenfield, Trends Anal. Chem. 18 (1999) 236.
[37] S. Hamdani, D. Joly, R. Carpentier, H.A. Tajmir-Riahi, J. Mol. Struct. 936 (2009) 80.
[38] Z. Vodrážka, D. Jandová, J. Grafnetterová, O. Schück, I. Kalousek, R. Tomášek, J. Lachmanová, Biochem. Pharmacol. 27 (1978) 1717.
[39] V. Panov, I. Shipanova, A. Michtchenko, I. Shabunin, N. Shimanovskii, L. Sibeldina, P. Sergeev, Biochem. Mol. Biol. Int. 35 (1995) 457.
[40] I. Shchipanova, V. Panov, S. Egorova, N. Shimanovskiĭ, P. Sergeev, L. Sibel'dina, Antibiot. Khimioter. 40 (1995) 8.
[41] S.M.M. Alam, L. Yeasmin, M.N. Reza, J.A. Shilpi, F. Ahmed, M.J. Akter, J. Biol. Sci. 4 (2004) 203.
[42] B.S. Liu, F.L. Zhao, C.L. Xue, J. Wang, Y.K. Lu, J. Lumin. 130 (2010) 859.
[43] F. Ding, G.Y. Zhao, S.C. Chen, F. Liu, Y. Sun, L. Zhang, J. Mol. Struct. 929 (2009) 159.
[44] X.M. He, D.C. Carter, Nature 358 (1992) 209.
[45] M.M. Tatli, G. Aktas, M. Kosecik, A. Yilmaz, Int. J. Antimicrob. Agents 21 (2003) 350.
[46] M. Dockal, D.C. Carter, F. Rüker, J. Biol. Chem. 274 (1999) 29303.